Directional and Frequency Spread of Surface Ocean Waves from CFOSAT/SWIM Measurements

Eva Le Merle, Danièle Hauser, C. Peureux, L. Aouf, Patricia Schippers, Christophe Dufour

HAL Id: insu-03379091
https://insu.hal.science/insu-03379091

Submitted on 15 Oct 2021

DIRECTIONAL AND FREQUENCY SPREAD OF SURFACE OCEAN
WAVES FROM CFOSAT/SWIM MEASUREMENTS

E. Le Merle [(1)], , D. Hauser [(1)], C. Peureux [(2)] , L. Aouf [(3)], P. Schippers [(4)]and C. Dufour [(5)]
(1) LATMOS (CNRS, Univ. Versailles Saint-Quentin, Paris Sorbonne Université), Guyancourt, France
(2) Collecte Localisation Satellite (CLS), Plouzané, France
(3) Météo-France, Toulouse, France
(4) ACRIS-ST, Guyancourt, France

ABSTRACT

The CFOSAT (China France Oceanography Satellite) mission launched in 2018 now routinely provides at the global scale, directional spectra of ocean waves. The principle is based on the analysis of the normalized radar cross-section measured by the instrument SWIM (Surface Waves Investigation and Monitoring), a near-nadir pointing Ku-Band real-aperture scanning radar. From the ocean wave spectra derived from SWIM, the principal parameters of ocean wave spectra as significant wave height, peak wavelength, and peak direction are now available to better characterize the sea-state. However, it is known that these principal parameters are not sufficient not fully characterize the distribution of wave energy and understand or validate the physical processes impacting its evolution during growth order decay. Here we show that the parameters characterizing the shape of the wave spectra (e.g directional and frequency spread) can be estimated at the global scale from the SWIM measurements. We also show that they can provide consistent values of the Benjamin-Feir index, an index proposed to estimate the probability of extreme waves. Similarities of differences with the shape parameters of the MFWAM numerical wave model are also discussed.

Index Terms— CFOSAT, SWIM, radar, ocean, ocean waves, ocean wave spectra

1. INTRODUCTION

Ocean surface waves are commonly described by their directional density spectrum of height, which characterizes the distribution of wave energy as a function of wave frequency (or wave number) and wave propagation direction. Apart from significant wave height, which is widely used to characterize or forecast the total energy of waves, the mean or peak period and the mean or peak directions are the most common parameters extracted and analyzed from these spectra. This reduces the information on directional spectra to only few parameters, whereas the directional or frequency spread are seldom analyzed. This limits the progress in the improvement of numerical wave models [1]. Indeed, several approximations are done in these models, such as the

discretized form of the non-linear wave-wave interactions, the angular distribution of wind input and wave dissipation. These assumptions may induce biases in the modeled wave spectra even if the total energy, characterized by the significant wave height is well reproduced. Another motivation for studying with more details the frequency and directional spread of the wave spectra is their link with the probability of occurrence of extreme waves. For example, [2] have shown the so-called Benjamin-Feir index (BFI) depends not only on the wave total energy but also on its distribution with frequency and direction.

SWIM is based on an original concept of near-nadir real-aperture radar, proposed in the 90's by Jackson et al [3] but implemented in space for the first tile with CFOSAT [4]. It provides directional spectra of ocean waves with wavelengths between 70 and 500m [4,5]. In [5], the performance on the wave height, dominant wave direction wavelength were analyzed. It was shown that except for waves which propagate in a ±15° sector along-track, the main parameters are in good agreement with the MFWAM model (French version of the WAM model of ECMWF) and *in situ* data.

In this paper, we go a step further by analyzing several parameters related to the frequency and angular distribution of the wave spectra obtained from the SWIM instrument. In section 2, we describe the SWIM and model data sets used in the analysis and recall the definition of the spectral parameters analyzed further below. We also present the wind and wave height conditions sampled in this study. In section 3, we present the spectral shape parameters (directional and frequency spread, BFI indexes) and discuss their geographic distributions and compare the results from SWIM and from MFWAM. We summarize and conclude in section 4.

2. DATA SETS AND METHODS

Ocean wave spectra from SWIM are those provided from the prototype processing chain in its V5.0.1. The products consist in 2D wave slope spectra sampled with 32 wavenumbers over the wavelength domain [70, 500] m and 12 directions every 15° in the range [0-180°], i.e. with a 180° ambiguity in the propagation direction. For the present analysis, we used the spectra obtained from the 10° incidence beam observations, and converted the 2D slope spectra into wave height spectra

expressed as a function of frequency (32 frequencies on the range [0.056, 0.26] Hz. For this conversion, we took the linear dispersion relationship in deep water. The processing version used here is based on the option#3 for the Modulation Transfer Function (see [4]) which means that the wave spectra are normalized so that the significant wave height is forced to be the same as the one estimate from the nadir-beam of SWIM.

SWIM wave spectral parameters are compared to parameters obtained from the MFWAM numerical model. This model is the French version of the third generation WAM model. It is based on the ECMWF version (ECW AM-IFS-38R2) with a parameterization taken from the WW3model [6]. The MFWAM products used here have a grid resolution of 10 km and are provided every 3-hours. The model is forced by winds from the IFS-ECMWF atmospheric system. Waves/currents interactions are taken into account with daily surface currents provided by the global PSY4-CMEMS ocean forecasting system. The MFWAM wave spectra are discretized in 24 directions every 15° between 0° and 360°, and 30 frequencies evenly spaced frequencies in the range [0.035- 0.58] Hz.
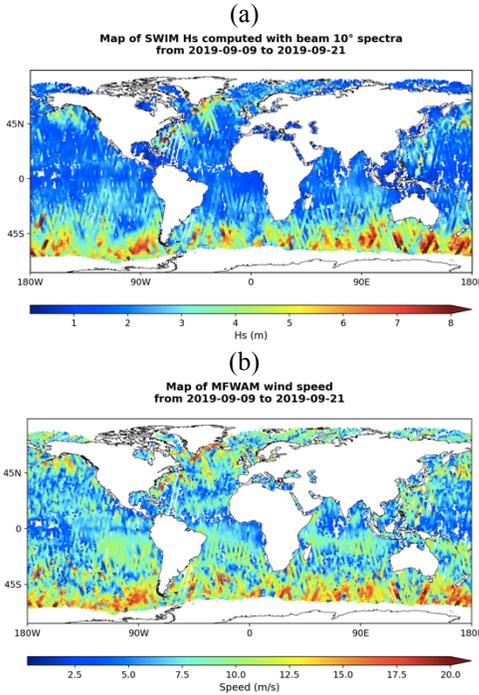
(a)

(b)

Fig.1 : Maps of (a) SWIM significant wave height (b) ECMWF wind speed plotted for the period 9-21 September 2019 at the locations of the SWIM measurements

In this study, we focus on a period of 13 days (a full orbital cycle of CFOSAT) between 9 and 21 September 2019. Figure 1 shows maps of the significant wave height from SWIM and of wind speed from MFWAM. During this period, high sea state conditions were encountered in the Southern Ocean with wind speed of more than 20 m/s and significant wave heights higher than 5m. These situations correspond to storms typical of the high latitudes in the Southern hemisphere where waves developing under high wind forcing are trapped within fast moving storms. The same kind of situation is also observed along the North American coasts where hurricane Humberto passed, and along the Greenland coasts where very an intense offshore wind event occurred.

In the following, three parameters are discussed to analyze the shape of the wave height spectra, namely the frequency width σ_f of the omnidirectional wave height spectrum E(f), the peakedness coefficient Q_p as defined by Goda [7], and the directional spread of σ_θ .

$$\sigma_f = \left[\int_{f_{min}}^{f_{max}} E(f) df \right]^2 / \int_{f_{min}}^{f_{max}} E^2(f) df \qquad (1)$$

$$Q_p = 2 \int_{f_{min}}^{f_{max}} f E^2(f) df \quad / \left[\int_{f_{min}}^{f_{max}} E(f) df \right]^2 \quad (2)$$

where E(f) is the omni-directional spectrum expressed as a function of frequency f.

$$\sigma_\phi = \sqrt{2 \left(1 - \sqrt{a_1(f)^2 + b_1(f)^2} \right)} \qquad (3)$$

where $a_1(f)$ and $b_1(f)$ are the first pair of the Fourier coefficients used to represent the directional distribution [9].

These parameters are estimated for both SWIM and MFWAM wave spectra by taking in both cases f_{min} and f_{max} as the limit of the SWIM frequency range ([0.056, 0.26 Hz]).

Two indexes for extreme waves characterization are also estimated, namely the BFI and BFI_2D as given by [2]:

$$BFI = k_0 \sqrt{m_0} \, Q_p \sqrt{2\pi} \qquad (4)$$

where k_0 is the mean wave number of the omnidirectional spectrum and m_0 its 0th order moment.

$$BFI_{2D} = BFI \left[1 + 7.10 \, \sigma_\phi^2 / 2 \, \omega_f^2 \right]^{-0.5} \qquad (5)$$

with $\omega_f = 1/(Q_p \sqrt{\pi})$

3. RESULTS

Figure (2a) shows the map of the frequency width σ_f estimated on the SWIM spectra. Compared to Fig.1a, it shows that regions corresponding to the smallest frequency width are generally those of the highest significant wave heights Hs. When plotting σ_f versus Hs (not shown) we find a clear decreasing trend. This behavior is also found on the WAM spectra (not shown). In opposite, when analyzed at the global scale, the relationship between σ_f and wave age (defined as Cp/U where Cp is the phase speed at the peak of the wave spectrum) is less clear.

Fig. 2b illustrates the histogram of SWIM-MFWAM differences for the σ_f parameter as a function of significant wave height. The overall agreement is very good with however a small negative bias at all Hs (-0.01 Hz) and rms error of 0.02 Hz. However, the scatter is significant for Hs
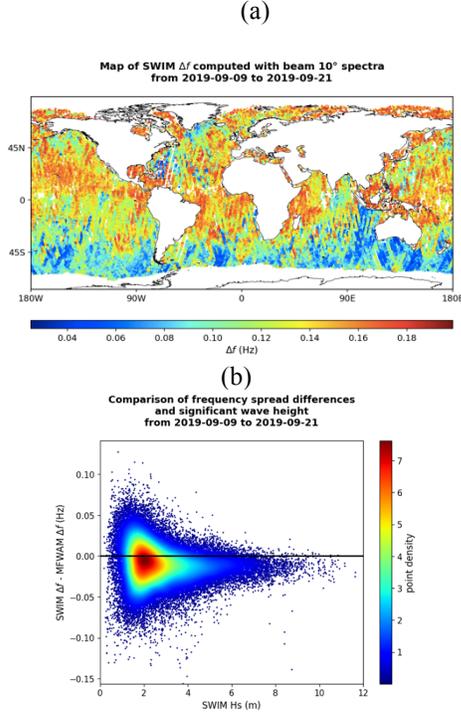
Fig.2 : (a) Map the parameter of spectral width sf deduced from the SWIM spectra.(b) histogram of the differences of sf valuesbetween SWIm and MFWAM as a function of the SWIM significant wave height.The data set is from 9 to 21 Sepetmber 2019.

less than about 1.5m (which correspond in the mean to $\sigma_f >$ 0.15 Hz). In these situations of low sea states, SWIM height spectra are perturbed by parasitic peaks at low wave numbers (see [5, 8]). Overall, MFWAM show largest values compared with SWIM. As suggested by [10], this overestimation by the model may be due to the approximations used in the representation of the non-linear save-wave interactions.

Figure 3 (a) shows the map of Qp parameter. The highest values of Qp are found in regions of extreme sea-state conditions mentioned in section 2. Compared to the case of σ_f, we find that Qp values are more clearly related to wave age with a clear negative trend for wave ages between 1 and 2 (not shown). Fig.(3b) shows the comparison between SWIM and MFWAM Qp values. It indicates that Qp is significantly larger for SWIM than for MFWAM, for all Hs > 1m. This indicates sharpest shapes of the omni-directional wave spectra. For Hs < 1m, the results from SWIM are much more scattered because of the difficulty to eliminate spurious peaks in the wave height omni-directional spectra (see [8]).

Figure (4a) shows the map of σ_ϕ, where σ_ϕ is estimated here at the frequency of the dominant waves (estimated for SWIM from the peak of the 2D wave slope spectra) . This map shows that the relationship between this parameter and sea-state conditions is not as clear as for σ_f or Qp. The most evident relationship is with the peak frequency or peak wavelength λ_p as shown in Fig. 4b for SWIM and 4c for MFWAM. Note that
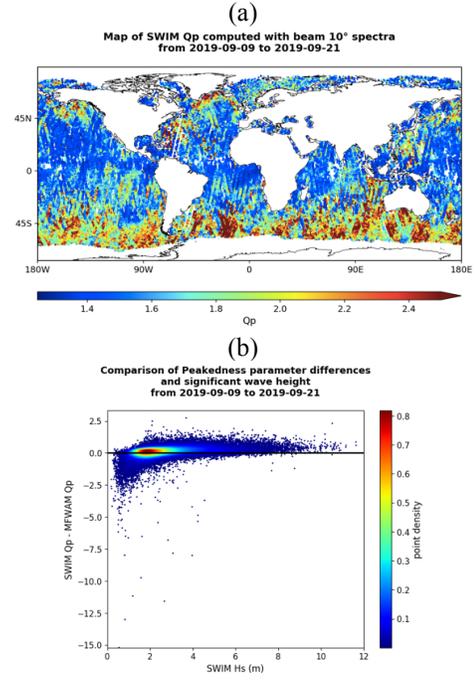

Fig.3 Same as in Fig.2 but for the parameter Qp.

in Fig.4c (MFWAM), there are two populations of points, not clearly apparent in Fig.4b (SWIM). This is due to a non continuous distribution of λ_p for MFWWAM with two maximum (around 120 m and 280 m). Nevertheless we can
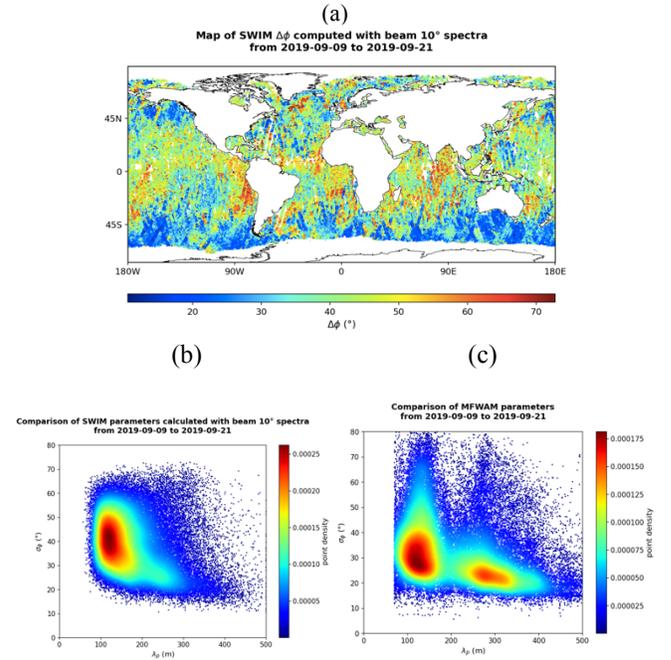

Fig.4 : (a)Same as in Fig2(a) but for the parameter of direcitonal spread sphi, (b-c) :corresponding histograms of the Qp values from SWIM (b) or MFWAM (c) as a function of the peak wavelength of SWIM (b) or MFWAM (c).

conclude from these figures that in both SWIM and MFWAM cases, the shortest wavelengths are associated to broader angular distributions. However, for the shortests wavelengths (70-150m) the most probable values of σ_ϕ are between 30° and 50° from SWIM , significantly larger than the MFWAM values (around 20°). For longest waves (around 200m), SWIM and MFWAM seem in better agreemnt with σ_ϕ values around 20°. Note that a 45° (resp. 20°) value for σ_ϕ corresponds to s ~ 2 (resp. s ~16) in a $\cos^{2s}$ angular distribution.

   Figure (5a) shows the map of the index BFI. It clearly shows that the highest values of BFI (i.e. > 0.4) are associated to the extreme sea-states in the Southern Ocean storms, and also close to the US coasts (related to the Humberto hurricanes) and to the Greenland coasts (related during this period to the high winds along-shore event). Fig. 5b shows the scatter plot of BFI for SWIM versus MFWAM. It shows that in the mean, BFI from SWIM is larger than from MFWAM. We could check that this difference is amplified in regions of high sea-state like in the Southern Ocean. When analyzing BFI_2D (not shown) we find the same kind of geographical distribution and a better agreement between SWIM and MFWAM. But this agreement is due a compensating effect of biases in Q_p or σ_θ and BFI (see (5) and results here-above.
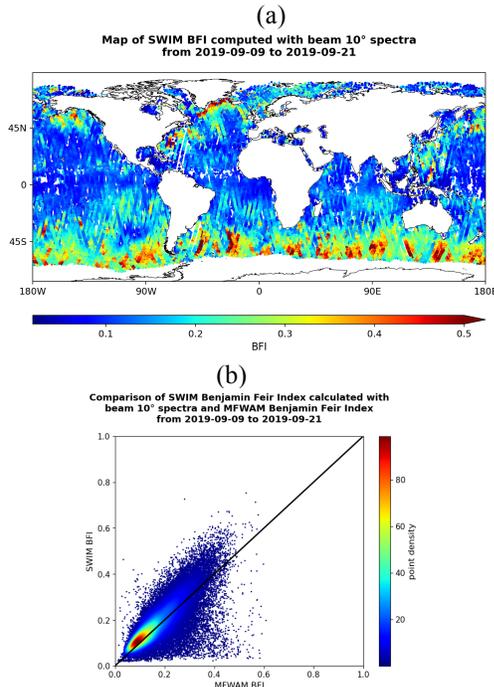
(a)

Map of SWIM BFI computed with beam 10° spectra
from 2019-09-09 to 2019-09-21

(b)

Comparison of SWIM Benjamin Feir Index calculated with
beam 10° spectra and MFWAM Benjamin Feir Index
from 2019-09-09 to 2019-09-21

Fig.5 : (a) Map of BFI from SWIM (b) Histogram of BFI
(SWIM versus MFWAM)

4. SUMMARY AND CONCLUSION

Here is presented an analysis of spectral shape parameters obtained from the observations of the SWIM instrument on-board CFOSAT. To our knowledge it is the first time that global statistics and maps of spectral shape parameters and BFI indexes are provided from observations. The order of magnitude of these parameters are consistent with what we know from previous studies and from models. Apart from cases with Hs < 1m, where SWIM data may be hampered by abnormal spectra at low significant wave height (Hs > 1), we can conclude that systematic biases between the MFWAM model and observations are found for the frequency width σ_f (smaller from SWIM), the peakedness parameter Qp (sharpest spectra for SWIM), and the angular spread of the dominant waves σ_ϕ (broader angular distribution for SWIM for the shortest dominant waves (70-150m). These biases induce biases in the BFI index. Because of compensating effects, BFI_2D from SWIM and MFWAM are however in a good agreement.

   Work is presently under progress to quality in more details these differences and try understand what are their origin.

REFERENCES

[1] D.T. Resio, L. Vincent, and D. Ardag, «Characteristics of directional wave spectra and implications for detailed-balance wave modeling », *Ocean Modelling, 103, 38-52,* 2016
[2] N. Mori, N., M. Onorato, M., P. A. E. M. Janssen, «On the estimation of the kurtosis in directional sea states for freak wave forecasting ». *Jour. Phys. Oceanogr., 41* , 1484-1497, 2011
[3] F. Jackson, F. C., Walton, W. T., Baker, P. L., «Aircraft and satellite measurement of ocean wave directional spectra using scannig-beam microwave radars» *Jour. Geophys.l Res. , 90(C1),* 987-1004. doi: 0148-0227/85/004C-1190$05.00 , 1985
[4] D. Hauser, Tison, C., Amiot, T., Delaye, L. et al, « SWIM: The first spaceborne wave scatterometer", *IEEE TGRS, 55(5),* 3000-3014, doi: 10.1109/TGRS.2017.2658672, 2017
[5] D. Hauser, D., Tourain, C., Hermozo, L. et al, «New observations from the SWIM radar on-board CFOSAT: Instrument validation and ocean wave measurement assessmen", *IEEE TGRS,* 5-26, doi: 10.1109/ TGRS.2020.2994372, 2020
[6] F. Ardhuin, F., E. Rogers, V. Babanin, et al., «Semi empirical dissipation source functions for ocean waves. Part I: Definition, calibration, and validation", *Jour. of Phys . Oceanogr., 40 (9),* 1917-1941, doi: 10.1175/2010JPO4324.1, 2010
[7] J-B. Saulnier,A. Clément, A. F.de O.Falcão, T. Pontes M. Prevosto, P. Ricci, « Wave groupiness and spectral band width as relevant parameters for the performance assessment of wave energy converters », *Ocean Engineering, 38,* 130–147 , 2011
[8] C. Tourain, D .Hauser et al, "Evolutions and improvements in CFOSAT SWIM Products", *Proceedings of IGARSS 2021,*
[9] M.S. Longuet-Higgins, D.E. Cartwright, D. (1963), "The directional spectrum of ocean waves, and processes of wave generation», *Proc. Royal Society of London. Series A, Mathematical and Physical Science*, 265 (1322), 286-315, 1963
[10] W. E. Rogers, G.P. Van Vledder, « Frequency width in predictions of windsea spectra and the role of the nonlinear solver », *Ocean Modelling 70*, 52–61, 10.1016/j.ocemod.2012.11.010, 2013